J Fluoresc (2014) 24:1215–1224
DOI 10.1007/s10895-014-1403-2

ORIGINAL PAPER

New spiro[benzotetraphene-fluorene] Derivatives: Synthesis and Application in Sky-Blue Fluorescent Host Materials

Jae-Ryung Cha · Chil-Won Lee · Myoung-Seon Gong

Received: 25 March 2014 / Accepted: 29 April 2014 / Published online: 25 May 2014

Abstract Blue light-emitting spiro[benzotetraphene-fluorene] (**SBTF**)-based host materials, 3-(1-naphthyl)-10-naphthylspiro[benzo*[ij]*tetraphene-7,9′-fluorene] (**1**), 3-(2-naphthyl)-10-naphthylspiro[benzo*[ij]*tetraphene-7,9′-fluorene] (**2**), and 3-[2-(6-phenyl)naphthyl]-10-naphthylspiro[benzo*[ij]*tetraphene-7,9′-fluorene] (**3**) were designed and prepared via multi-step Suzuki coupling reactions. Introducing various aromatic groups into **SBTF** core lead to a reduction in band gap and a determination of the color purity and luminescence efficiency. Typical sky-blue fluorescent organic light emitting diodes with the configuration of ITO/*N,N′*-di(1-naphthyl)-*N,N′*-bis[(4-diphenylamino)phenyl]-biphenyl-4,4′-diamie (60 nm)/*N,N,N′,N′*-tetra(1-biphenyl)-biphenyl-4,4′-diamine (30 nm)/host: dopant (30 nm, 5 %)/LG201 (electron transporting layer, 20 nm)/LiF/Al were developed using **SBTF** derivatives as a host material and *p*-bis(*p*-*N,N*-diphenyl-aminostyryl)benzene (**DSA-Ph**) as a sky-blue dopant material. A device obtained from three materials doped with **DSA-Ph** showed color purity of 0.148 and 0.239, a luminance efficiency of 7.91 cd/A, and an external quantum efficiency >4.75 % at 5 V.

Keywords Fluorescence blue OLED · Sky blue · Spiro[benzotetraphene-fluorene] · Color purity

J.-R. Cha · M.-S. Gong (✉)
Department of Nanobiomedical Science and BK21 PLUS NBM Global Research Center, Dankook University, Chungnam 330-714, Republic of Korea
e-mail: msgong@dankook.ac.kr

C.-W. Lee
Department of Polymer Science and Engineering, Dankook University, 126, Jukjeon-dong, Suji-gu, Yongin, Gyeonggi 448-701, Republic of Korea

Introduction

Many blue light-emitting dyes have been studied to achieve stability, efficiency, and color purity [1–3]. In particular, a high efficient blue light-emitting material needs to be developed to reduce organic light-emitting diode (OLED) power consumption and increase the color range [4]. However, it is difficult to design blue light-emitting materials with high efficiency and saturated color purity due to the wide band gap.

Anthracene plays an important role in the development and application of OLED materials such as blue-emitting materials and hole- and electron-transporting materials. Their derivatives have been reviewed and discussed in relation to thermal stability and electroluminescent performance [5–9].

Spirobifluorene derivatives have received a great deal of attention, because they preserve the inherent characteristics of spiro compounds such as morphological stability, high glass transition temperature, and amorphous properties [10–15]. Spiro[benzo*[c]*fluorene-7,9′-fluorene] (**SBFF**) can be substituted with a variety of substituents because of the asymmetrical spiro core structure. Therefore, conjugation length and color characteristics can be controlled as a host material as shown in Scheme 1 [16–21].

Architecture of more fused π-conjugated spiro molecules has been extensively studied because of their various applications in OLEDs. The unique structure of highly conjugated spiro molecules has allowed their optical and electrochemical properties to be delicately tuned over a wide range by appropriate chemical modification to the aromatic moieties. Spiro[benzoanthracene-7,9′-fluorene] (**SBAF**) derivatives have been prepared and adopted to fluorescent host and dopant materials [22, 23]. In the course of studying the fused-ring aromatic spiro molecules, the benzotetraphene structure was incorporated into the spiro structure to endow more conjugation and versatile substituents.

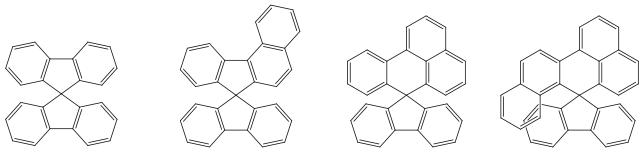

Scheme 1 Various spiro-core molecules: **SBF**, spirobifluorene; **SBFF**, spiro[benzo*[c]*fluorene-7,9′-fluorene]; **SBAF**, spiro[benzo*[de]*-anthracene-7,9′-fluorene]; **SBTF**, spiro[benzo*[ij]*tetraphene-7,9′-fluorene]

The color purity and luminescence efficiency performance of OLEDs based on **SBTF** could be expected by the substitution positions and a variety of aryl moieties with a variety of conjugation chain lengths [24].

In this study, a novel tetraphene derivative with a spiro[benzotetraphene-fluorene] (**SBTF**) core structure was developed as a high fluorescent blue host material with good thermal/morphological stability, and its physical properties were investigated. Three new blue host materials consisting of **SBTF** and various aromatic substituents were prepared and characterized using ^{1}H nuclear magnetic resonance (NMR), ^{13}C NMR, Fourier transform-infrared spectroscopy (FT-IR), mass spectroscopy, thermal analysis, UV–vis, and photoluminescence spectroscopy. The EL properties of multilayered sky-blue OLEDs fabricated using three host materials and **DSA-Ph** as the dopant were evaluated.

Experimental

Materials and Measurements

Tetrakis(triphenylphosphine)palladium(0), (Aldrich Chem. Co., St. Louis, MO, USA), 2-(6-phenyl)naphthyl boronic acid, naphthalene-1-boronic acid and naphthalene-2-boronic acid (Frontier Scientific Co., West Logan, UT, USA) were used as received. 8-[2-[6-(2-naphthyl)]] naphthyl-1-bromonaphthalene was prepared by a successive Suzuki reaction using corresponding organic boronic acids and halides. **DSA-Ph** was adopted as the sky-blue dopant material (HOMO=5.40 eV; LUMO=2.70 eV). *n*-Butyllithium (2.5 M solution in hexane), potassium carbonate, sodium hydroxide and HCl (Duksan Chem. Co., Seoul, South Korea) were used without further purification. Tetrahydrofuran (THF) was purified by distillation over sodium metal and calcium hydride. Photoluminescence (PL) spectra were recorded on a fluorescence spectrophotometer (Jasco FP-6500; Tokyo, Japan) and UV-Vis spectra were obtained by a UV-Vis spectrophotometer (Shimadzu, UV-1601PC; Tokyo, Japan). Energy levels were measured with a low-energy photo-electron spectrometer (AC-2; Riken-Keiki, Union City, CA, USA). FT-IR spectra were obtained with a Thermo Fisher Nicolet 850 spectrophotometer (Waltham, MA, USA), and elemental analyses were performed using CE Instrument EA1110 (Hindley Green, Wigan, UK). Differential scanning calorimeter (DSC) measurements were performed on a Shimadzu DSC-60 DSC under nitrogen. The thermogravimetric analysis (TGA) measurements were performed on a Shimadzu TGA-50 thermo gravimetric analyzer. High resolution mass spectra were recorded using an HP 6890 (Brea, CA, USA) and Agilent Technologies 5975C MSD in FAB mode (Palo Alto, CA, USA).

Preparation of 10-naphthylspiro[benzo*[ij]* tetraphene-7,9′-fluorene] (**NSBTF**)

A solution of 8-[2-[6-(2-naphthyl)]]naphthyl-1-bromonaphthalene (14.06 g, 30.6 mmol) in THF (100 mL) was added to a 250 mL two-necked flask. The reaction flask was cooled to −78 °C, and *n*-BuLi (2.5 M in *n*-hexane,14.68 mL) was added slowly in a dropwise fashion. The solution was stirred at this temperature for 1 h, followed by adding a solution of 9-fluorenone (5.51 g, 30.6 mmol) in THF (30 mL) under an argon atmosphere. The resulting mixture was gradually warmed to ambient temperature and quenched by adding saturated aqueous $NaHCO_3$ (90 mL). The mixture was extracted with dichloromethane. The combined organic layers were dried over magnesium sulfate, filtered, and evaporated under reduced pressure. A yellow powdery product was obtained. The crude residue was placed in another two-necked flask (100 mL) and dissolved in acetic acid (50 mL). A catalytic amount of aqueous HCl (5 mol%, 12 N) was then added, and the whole solution was heated under reflux for 12 h. After cooling to ambient temperature, the compound was purified as a white powder by silica gel chromatography using dichloromethane/*n*-hexane (2/1).

10-Naphthylspiro[benzo*[ij]*tetraphene-7,9′-fluorene] (**NSBTF**, 5.42 g, 10 mmol) was dissolved in carbon tetrachloride in a two-necked flask; bromine (2.36 g, 15 mmol) was then added slowly in a dropwise fashion over a period of 20 min. The mixture was stirred at room temperature for 3 days. The precipitated solid was filtered and dried *in vacuo* to give the crude product, which was purified by recrystallization from ethyl acetate/*n*-hexane (1/2) to give a white powder.

NSBTF: yield 86 %. Mp 333 °C. UV-vis (THF): λ_{max} (absorption)=362, 379 nm, λ_{max} (emission)=396, 415 nm. ^{1}H NMR (500 MHz, $CDCl_3$, ppm) 8.46–8.32 (2d, 2H), 8.0–7.40 (m, 15H), 7.25–7.06 (m, 6H), 6.99–6.57 (2d, 2H). ^{13}C NMR (500 MHz, $CDCl_3$, ppm) 150.4, 148.1, 147.4, 142.8,

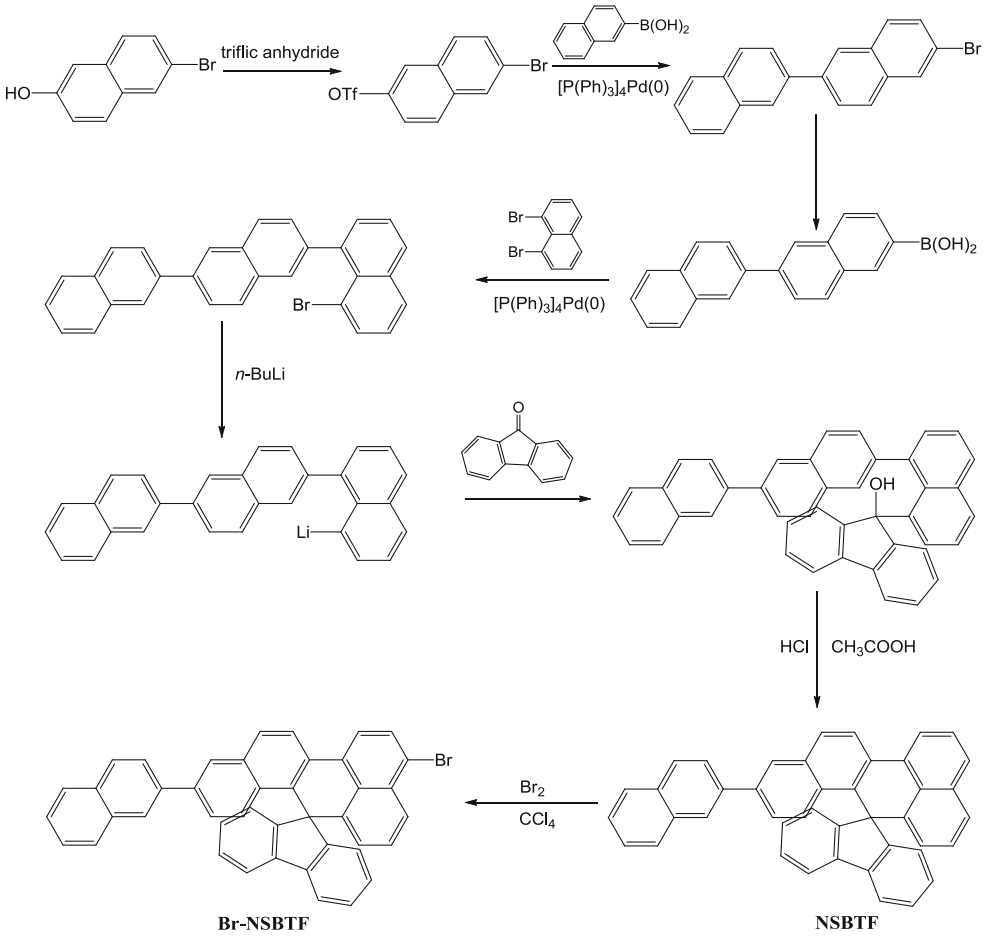

Scheme 2 Synthetic routes of 10-naphthylspiro[benzo*[ij]*tetraphene-7,9′-fluorene] core

142.2, 140.0, 139.2, 138.4 137.8, 137.2, 136.8, 136.2, 135.2, 134.4, 133.8, 133.2, 130.7, 129.6, 129.2, 128.2, 128.0, 127.8, 127.4, 126.2, 125.8, 125.2, 124.4, 124.0, 123.3, 122.8, 122.4, 120.4, 120.1, 66.5. FT-IR (KBr, cm^{-1}) 3060, 3040, 3018 (aromatic C–H). Anal. Calcd. for $C_{43}H_{26}$ (542.67): C, 95.17; H, 4.83. found: C, 95.20; H, 4.85. MS (FAB) m/z 543.20 $[(M+1)^+]$.

Representative Preparation of 3-(1-naphthyl) -10-naphthylspiro[benzo*[ij]*tetraphene-7,9′-fluorene] (**1**)

A solution of 3-bromo-10-naphthylspiro[benzo*[ij]*tetraphene-7,9′-fluorene] (6.22 g, 10 mmol), tetrakis (triphenylphosphine)palladium(0) (0.59 g, 0.51 mmol), and naphthalene-1-boronic acid (1.72 g, 10 mmol) dissolved

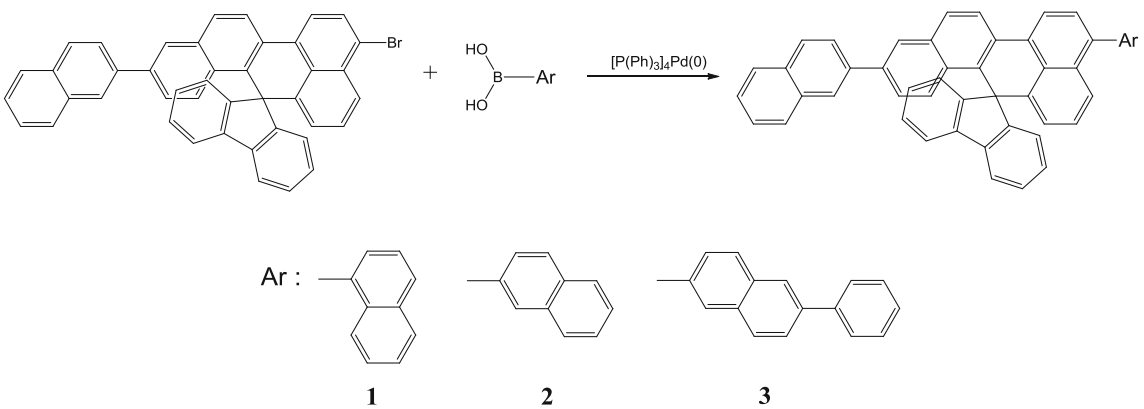

Scheme 3 Preparation of three **NSBTF** derivatives

Table 1 UV absorption, PL, energy levels and thermal properties of **NSBTF** hosts

Sample properties			**NSBTF**	**1**	**2**	**3**
Purity[a]	HPLC	(%)	99.9	99.9	99.9	99.9
Thermal analysis	DSC	T_g (°C)	145	194	179	183
		T_m (°C)	333	368	322	356
Optical analysis	UV (THF)	Max (nm)	362, 379	363, 383	370, 387	375
		Bg[b] (eV)	3.15	3.09	3.00	2.98
	PL (THF)	Max (nm)	396,415	413,431	442	447
		FWHM[c] (nm)	41	53	43	61
	PL (Film)	Max (nm)	412	425	445	448
		FWHM[c] (nm)	52	56	58	61
Electrical analysis	AC-2[d]	HOMO (eV)	5.88	5.88	5.82	5.80
		LUMO (eV)	2.73	2.79	2.82	2.82

[a] The purity of the samples were finally determined by high performance liquid chromatography (HPLC) using the above prepared samples after train sublimation

[b] Bandgap

[c] Full width at half maximum

[d] AC-2(60 nm film)

in THF (150 mL) was stirred in a double-necked flask for 30 min. Potassium carbonate (2 M, 150 ml) was added dropwise over 20 min. The resulting reaction mixture was refluxed overnight at 80 °C and then extracted with ethyl acetate and water. After the organic layer was evaporated with a rotary evaporator, the resulting powdery product was purified by column chromatography from dichloromethane/*n*-hexane (1/1) to give the yellow crystalline product **1**. Other **SBTF** hosts **2** and **3** were prepared using similar procedures described above.

1: yield 78 %. Mp 368 °C. UV-vis (THF): λ_{max} (absorption)=363 and 383 nm, λ_{max} (emission)=413 and 431 nm. ^{1}H NMR (500 MHz, $CDCl_3$, *ppm*) 8.54–8.44 (2d, 2H), 8.05–7.23 (m, 22H), 7.17–7.10 (m, 6H), 6.95 (t, 1H), 6.59 (d, 1H). ^{13}C NMR (500 MHz, $CDCl_3$, ppm) 152.1, 150.6, 148.6, 148.0, 147.4, 143.2, 142.6, 142.2, 141.3, 140.2, 139.4, 138.8, 137.6, 137.0, 136.8, 135.2, 134.2, 133.8, 133.4, 130.7, 129.8, 129.2, 128.6, 128.2, 127.6, 127.2, 126.5, 125.9, 125.2, 124.5, 124.0, 123.6, 123.0, 122.7, 120.6, 120.2, 66.6. FT-IR (KBr, cm^{-1}) 3060, 3038, 3018 (aromatic C–H). Anal. Calcd. for $C_{53}H_{32}$ (668.82): C, 95.18; H, 4.82. Found: C, 95.09; H, 4.81. MS (FAB) m/z 669 [$(M+1)^+$].

2: yield 81 %. Mp 322 °C. UV-vis (THF): λ_{max} (absorption)=370, 387 nm, λ_{max} (emission)=442 nm. ^{1}H NMR (500 MHz, $CDCl_3$, *ppm*) 8.52–8.42 (2d, 2H), 8.04–7.41 (m, 22H), 7.25–7.06 (m, 7H), 6.63 (d, 1H).^{13}C NMR (500 MHz, $CDCl_3$, ppm) 152.0, 150.6, 148.8, 148.2, 147.5, 146.2, 144.6, 143.2, 142.5, 142.0, 141.4, 140.2, 139.5, 138.8, 137.5, 137.0, 136.6, 135.1, 134.2, 133.6, 133.2, 130.8, 129.4, 129.0, 128.6, 128.1, 127.6, 127.2, 126.6, 125.8, 125.2, 124.4, 123.8, 123.2, 122.8, 120.8, 120.2, 66.5. FT-IR (KBr, cm^{-1}) 3060, 3018 (aromatic C-H). Anal. calcd. for $C_{53}H_{32}$ (668.82): C, 95.18; H, 4.82. Found: C, 95.09; H, 4.81. MS (FAB) m/z 669 [$(M+1)^+$].

3: yield 76 %. Mp 356 °C. UV-vis (THF): λ_{max} (absorption)=375 nm, λ_{max} (emission)=447 nm. ^{1}H NMR (500 MHz, $CDCl_3$, *ppm*) 8.52–8.42 (2d, 2H), 8.15–7.41 (m, 26H), 7.22–7.05 (m, 6H), 6.64 (d, 1H). ^{13}C NMR (500 MHz, $CDCl_3$, ppm) 151.1, 150.6, 148.2, 148.0, 147.6, 143.2, 142.7, 142.1, 140.2, 138.8, 137.6, 137.0, 136.9, 136.5, 135.2, 134.3, 133.9, 133.5, 133.0, 130.8, 129.5, 129.0, 128.7, 128.2, 127.8, 127.4, 127.2, 126.7, 126.2, 125.8, 125.4, 125.0, 124.6, 124.0, 123.7, 123.2, 122.6, 122.0, 120.7, 120.2, 66.4. FT-IR (KBr, cm^{-1}) 3060, 3018 (aromatic C–H). anal. calcd. for $C_{59}H_{36}$ (744.28): C, 95.13; H, 4.87. Found: C, 95.09; H, 4.84. MS (FAB) m/z 745.28 [$(M+1)^+$].

OLED Fabrication

A basic device configuration of indium tin oxide (150 nm)/*N,N′*-di(1-naphthyl)-*N,N′*-bis[(4-diphenylamino)phenyl]-biphenyl-4,4′-diamie (DNDPB, 60 nm)/*N,N,N′,N′*-tetra(1-biphenyl)-biphenyl-4,4′-diamine (TBB, 30 nm)/**SBTF hosts: DSA-Ph** (30 nm, 5 %)/LG201 (20 nm)/LiF (1 nm)/Al (200 nm) was used for device fabrication. The organic layers were deposited sequentially onto the substrate at a rate of 1.0 Å/s by thermal evaporation from heated alumina crucibles. The concentration of the dopant materials was varied at 5 %. The devices were encapsulated with a glass lid and a

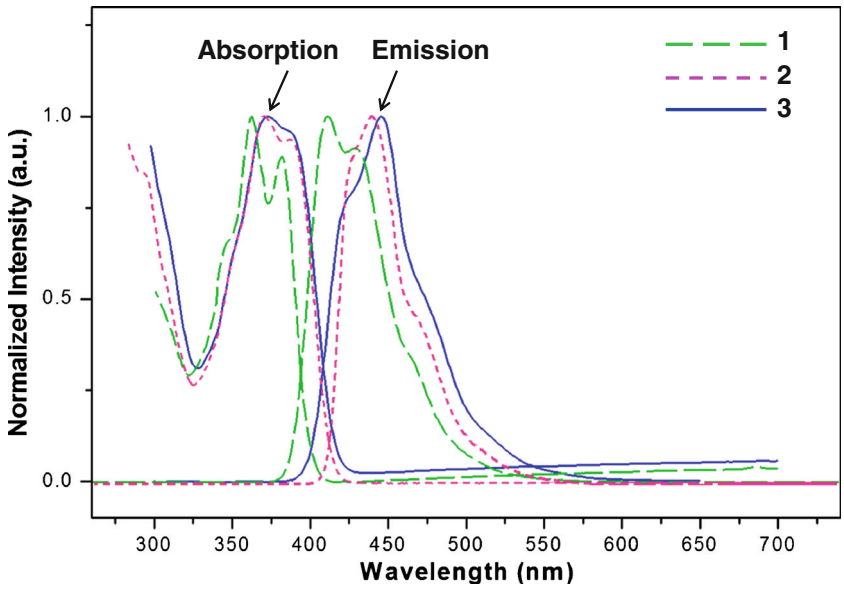

Fig. 1 UV-Vis and PL spectra of **NSBTF** host materials

CaO getter after cathode deposition. Current density—voltage luminance and EL characteristics of the blue fluorescent OLEDs were measured with a Keithley 2400 source measurement unit (Cleveland, OH, USA) and a CS 1000 spectroradiometer.

Results and Discussion

Synthesis and Characterization

8-[2-[6-(2-Naphthyl)]]naphthyl-1-bromonaphthalene was prepared by multi-step reactions including selective Suzuki C-C coupling as shown in Scheme 1: 1) triflation, 2) selective introduction of naphthyl group to the 6-position of 2-bromonaphthalene, 3) boration, 4) C-C coupling with 1,8-dibromonaphthalene via the Suzuki reaction, 5) spiro-formation of 8-[2-[6-(2-naphthyl)]]naphthyl-1-bromonaphthalene with 9-fluorenone via lithiation, followed by six-membered ring formation by acid catalyzed cyclization. Selective bromination of **NSBTF** at the 3-position was performed in carbon tetrachloride solvent. The molecular structures of the various aromatic group-substituted **NSBTF** derivatives and their synthetic routes are illustrated in Scheme 2 and Scheme 3. These compounds can be obtained with moderate yields. The chemical structures and composition of the resulting precursors and spiro-compounds were characterized by ^{1}H NMR, ^{13}C NMR, FT-IR, gas chromatography-MS, and elemental analysis.

Thermal Properties

The thermal stability of organic materials is crucial to the stability and lifetime of the OLED devices. Degradation of OLEDs depends on the morphological changes resulting from the thermal stability of the amorphous organic layer. A high glass transition temperature (T_g) value indicates that the morphology of the material will not easily be changed by the high temperatures generated during the operation of OLED devices [25, 26]. The thermal properties of the newly synthesized host

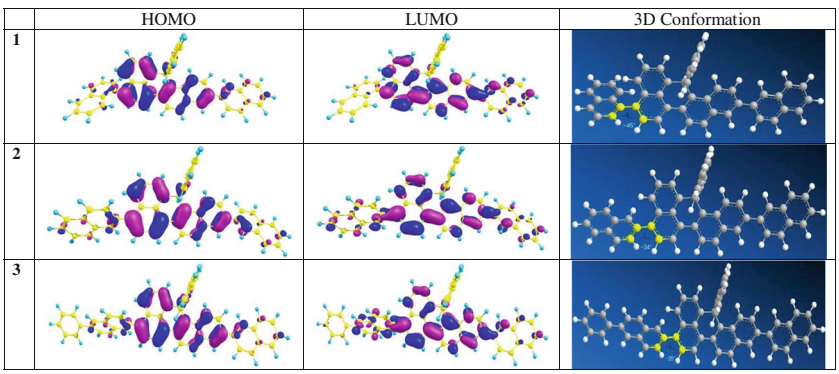

Fig. 2 HOMO and LUMO electronic density distributions of four **NSBTF** host materials, calculated at the DFT/B3LYP/6-31G* for optimization and Time Dependent DFT (TDDFT) using Gaussian 03

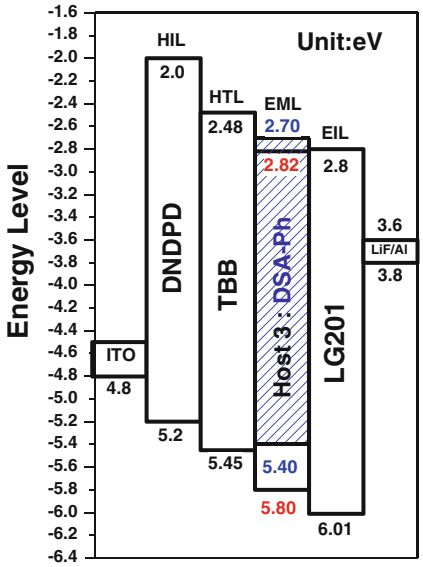

Fig. 3 Energy diagram of the sky-blue fluorescence devices using **NSBFF** host material **4**

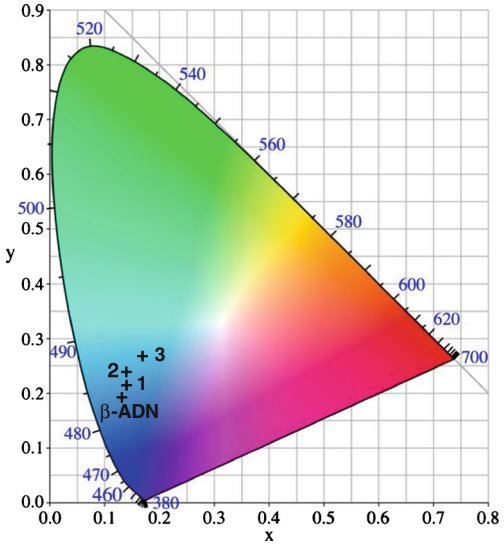

Fig. 5 CIE coordinations for the **NSBTF** and **β-ADN** host materials

materials were investigated by DSC and TGA. The onset decomposition temperatures were >450 °C for the three host materials, which is summarized in Table 1. The purified samples of **1**, **2**, and **3** showed melting points (T_m) of 368, 322 and 356 °C, respectively. No melting points were observed during the second heating, even though the sample was given enough time to cool in air. Once the sample became an amorphous solid, it did not revert to the crystalline state. After the sample had cooled to room temperature, a second DSC scan performed at 10 °C/min revealed T_g at 194, 179 and 183, respectively, which were much higher than that of MADN (120 °C). As a result, the amorphous glassy state films of the three host materials were good candidates as EL materials [27].

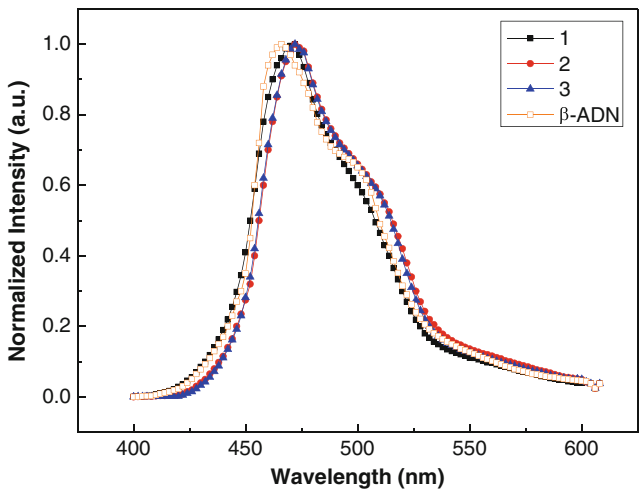

Fig. 4 Electroluminescence spectra of the blue fluorescence devices using **NSBTF** host materials

Optical Properties and Energy Levels

Figure 1 shows the absorption and fluorescence spectra of the three host materials in dilute THF solution. Absorption spectra of **1** and **2** with two maximum peaks were similar except for the absorption edge of the UV-vis spectra. The same **NSBTF** core and naphthalene side group were used in the molecular structure and similar absorption spectra were obtained. The difference of the absorption edge in the two host materials is due to the steric hindrance of the 3-naphthyl group in the host **1**. Three compounds exhibited typical blue emission in solution with a maximum peak of about 440 nm. The photophysical properties of these compounds are summarized in Table 1.

Solution **1** had UV maximum absorption peaks at 363 and 383 nm and blue emission of about 413 and 431 nm. However, **3** had a maximum absorption of 375 nm and an emission of 447 nm, indicating a red shift of about 10–15 nm relative to **1**. Introducing a phenylnaphthyl group to the 3-position in **3** caused a red-shift in the absorption and emission spectra even as conjugation length increased. The PL spectrum of **1** was also blue shifted due to the reduced conjugation length of the naphthalene in the host **1**.

A molecular simulation of three **NSBTF** hosts was carried out to understand the physical properties at the molecular level. Figure 3 shows the geometric structure of **1**, **2** and **3**. The 3-naphthyl and **NSBTF** core in **2** and **3** can be freely rotated, but the rotation of the 3-naphthyl and **NSBTF** core in **1** is limited by the steric hindrance of the spirobifluorene with the naphthalene. This leads to the distortion of the naphthalene substituent and the conjugation of the naphthalene can be destroyed by the **NSBTF** group in **1** [28].

Molecular simulation also showed the electron distribution of the three **NSBTF** host materials. The highest

Table 2 Eelectroluminescence properties of the devices obtained from **NSBTF** hosts and **DSA-Ph** dopant materials

Properties	Host Dopant	**1** DSA-Ph	**2**	**3**	β-ADN
	(%)	5 %			
EL at 5 V	λ_{max} (nm)	472	472	471	466
	FWHM (nm)	58	56	58	57
	mA/cm^2	11.87	14.58	13.23	7.54
	cd/A[a]	6.27	7.27	7.91	5.90
	cd/A[b]	6.96 (3.9 V)	7.47 (3.9 V)	8.03 (4.5 V)	6.8 (7 V)
	cd/m^2	715	907	809	550
	CIE-x	0.148	0.151	0.148	0.149
	CIE-y	0.204	0.245	0.239	0.215
	EQE(%)[a]	4.25	4.35	4.76	3.94

[a] Values at 5 V

[b] Values at a highest peak

occupied molecular orbital (HOMO) and the lowest unoccupied molecular orbital (LUMO) distribution of **1**, **2** and **3** are shown in Fig. 2. The HOMO and LUMO orbitals were concentrated in the **SBTF** core, and substitution of fluorene affect slightly the HOMO and LUMO distribution in the host materials.

The energy levels of the three host materials used to fabricate the OLEDs are shown in Fig. 3. As seen in the molecular structure of the **1**, the naphthyl group substituted at 4-position can be distorted by the **NSBTF** core, leading to the reduction of the degree of conjugation of the **NSBTF**. The distortion of the conjugated structure of the **NSBTF** increases the bandgap for **1** compared with **2**, leading to the blue shift of the absorption edge of the UV-vis spectrum.

Energy gaps for **1**, **2**, and **3** and **DSA-Ph** were calculated as 3.09, 3.00, 2.98 and 2.58 eV, respectively. The highly conjugated host **3** had the lowest band gap of 2.98 eV. The HOMO energy levels were −5.88, −5.82, −5.80, −5.85 and 5.48 eV for **1**, **2**, **3** and **DSA-Ph**, respectively. The HOMO values of **1**, **2** and **3** were similar to those of other commercial anthracene derivatives (−5.5 to −6.0 eV) such as 2-methyl-9,10-di(2-naphthyl)anthracene and 9,10-di(2-naphthyl)anthracene (**β-ADN**) [4].

EL Properties

The EL spectra of the blue fluorescent **SBTF** devices doped by the **DSA-Ph** dopant at concentrations of 5 % are shown in

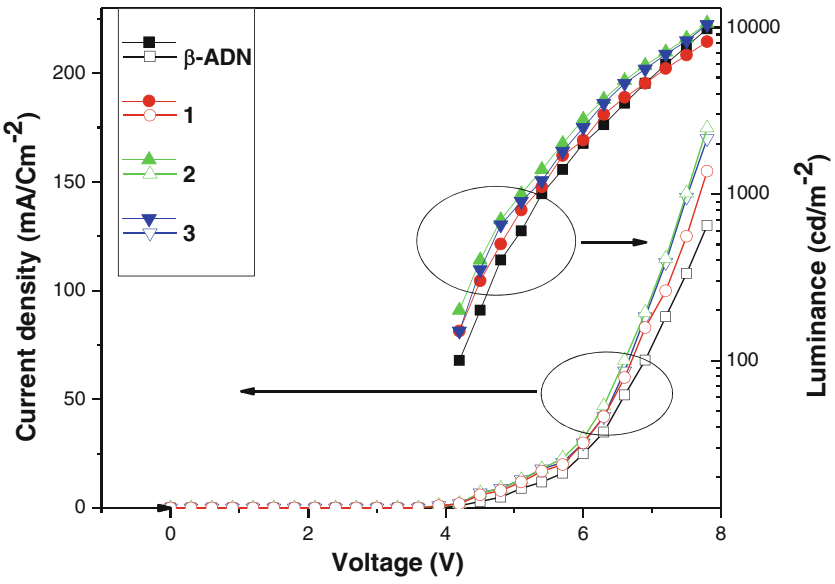

Fig. 6 Current density-voltage-luminescence characteristics of the devices using **NSBFF** host materials doped with 5 % **DSA-Ph**

Fig. 4 and showed a maximum peak at 472 nm for **1**, **2** and **3**, and 466 nm for **β-ADN**. Sky blue emission was observed, and the color coordinates of the device **3** were about 0.148 and 0.239. The EL spectra of the three host materials were slightly different from that of **β-ADN**, as summarized in Fig. 5 and Table 2. The peak EL spectra was also 472 nm, and the spectra were consistent with even substitution of different aromatic groups to the **SBTF** ring. The EL emission was dominated by the emission peak of the dopant, suggesting that the energy transfer from the host to **DSA-Ph** dopant was quite efficient at the optimum dopant concentration employed in this experiment. The full width at half maximum (FWHM) of 55–58 nm was relatively constant, which lead to sky blue, as illustrated in the PL spectrum (41–61 nm). Based on the difference and shape FWHM between the PL and EL spectra, we conclude that the blue EL was due to the emission of **NSBTF** host materials, with emission interference from the dopant.

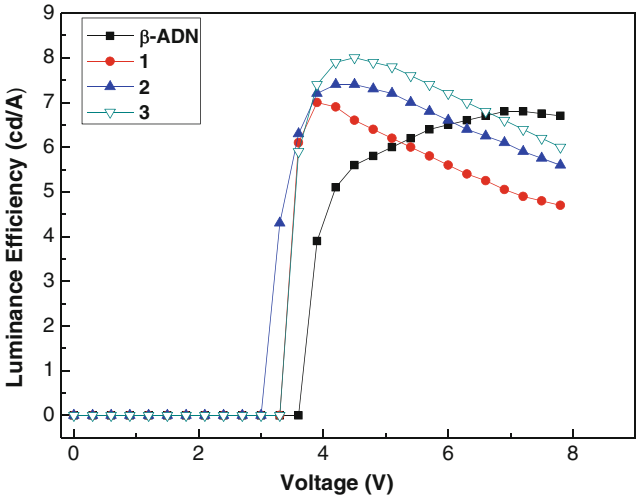

Fig. 7 Luminance efficiency-voltage characteristics of the device using **NSBTF** host materials

OLED Device Properties

The EL properties of the three **NSBTF** hosts and commercial **β-ADN** host materials were examined by fabricating multilayer devices with the following configuration: glass ITO anode/hole injection layer (HIL)/hole transfer layer (HTL)/emitting layer (EML)/electron transport layer (ETL)/LiF (EIL)/Al cathode. DNDPD was used as the HIL, TBB as the HTL, host: 5 % dopant as the EML and LG201 as the ETL; A 10 Å LiF layer was used as the EIL. **NSBTF** derivatives **1**, **2** and **3** and commercial **β-ADN** were evaluated as host materials for sky-blue fluorescent OLEDs. **DSA-Ph** was used as the sky-blue dopant and the device performance of the blue OLEDs was studied. Figure 6 shows the luminance–voltage–current density characteristics of the OLEDs with three hosts and 5 % **DSA-Ph** dopant. Although host **2** has a band gap of 3.0 eV, they showed a slightly higher current density and luminance than those of other hosts including **β-ADN** at the same driving voltage. The decrease of the current density and luminance in the **1** device is originated from the wide bandgap of **1**. The HOMO level of **1** was 5.88 eV compared with 5.82 eV of 2, while the LUMO level of **1** was similar to that of **2**. The deep HOMO level of the **1** hinders the hole injection from the TBB hole transport layer to the emitting layer due to the large energy barrier for hole injection, leading to low current density and low luminance [29].

As shown in the luminance efficiency curves of the three devices in Fig. 7, high efficiencies >7.91 cd/A were obtained for the **3** device as summarized in Table 2. All devices exhibited moderate current density before the turn-on voltage because of the absence of a shunt resistance. Although the CIE value of the **3** device was different from that of the **β-ADN** device, its luminance efficiency was much higher than that of the **β-ADN** device, which was 5.9 cd/A at 5 V. In the case of the device **3** doped with 5 % **DSA-Ph**, the maximum brightness of 350 cd/m^2 and 8.03 cd/A occurred at a low driving voltage of 4.5 V.

The maximum quantum efficiency of the device obtained from the three devices was an external quantum efficiency (EQE) of 4.76 % and efficiency increased rapidly to a maximum of approximately 7.91 cd/A at a low current density of 11.87 mA/cm^2 at 5 V as shown in Fig. 8. **NSBTF** hosts doped with 5 % **DSA-Ph** showed a small decrease in efficiency as the current density was increased, i.e., a weak-current-induced fluorescent quenching [30].

The holes injected from a hole transfer layer were transferred to the lighting emitting layer and were trapped at dopant sites. The sky-blue styrylarylene-type dopant **DSA-Ph** had a large capacity to catch the holes, and minimized the loss of holes resulting in good EL efficiency. Thus, the HOMO level

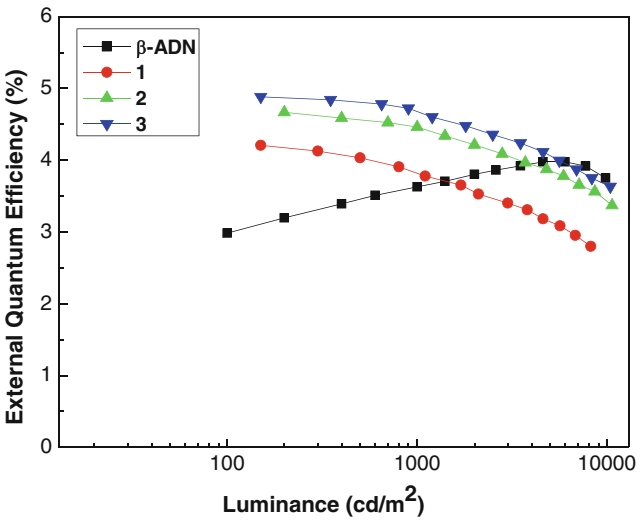

Fig. 8 Quantum efficiency–luminance curves of the **NSBTF** host materials

of **DSA-Ph** was suitable for hole trapping and hole transporting as a dopant, and the **MSBTF** hosts were moderate for balancing holes and electrons in the emitting layer. In the fluorescent host-dopant system, the probability of energy transfer from the excited energy donor to the energy acceptor depends on the overlap of the emission spectrum of the donor with the absorption spectrum of the acceptor. This is evident from the spectral overlap between the PL of **NSBTF** and the UV absorption of **DSA-Ph** [31, 32].

Combined good efficiency and color purity enabled the non anthracene-type fused ring spirotetraphene derivatives to be good candidates as sky blue emitters for OLEDs.

Conclusion

New fluorescence blue host materials based on **SBTF** derivatives were successfully prepared and used to construct blue OLEDs. Substitution of the aromatic group on the 3-position of **NSBTF** core distorted the conjugated structure little and improved T_g for good thermal stability. The EL emission spectra of the devices were about 472 nm. The typical OLED devices showed excellent performance; the **NSBTF**-based device exhibited highly efficient blue-light emission with a maximum efficiency of 7.91 cd/A (EQE, 4.75 %) at 5 V. According to these characteristics, these blue light emitting materials have sufficient potential for fluorescent OLED applications.

References

1. Gao ZQ, Mi BX, Chen CH, Cheah KW, Cheng YK, Wen WS (2007) High-efficiency deep blue host for organic light-emitting devices. Appl Phys Lett 90:123506–123508
2. Lee MT, Chen HH, Lian CH, Tsai CH, Chen CH (2007) Stable styrylamine-doped blue organic electroluminescent device based on 2-methyl-9,10-di(2-naphthyl)anthracene. Appl Phys Lett 85:3301–3303
3. Tao S, Hong Z, Peng Z, Ju W, Zhang X, Wang P, Wu S, Lee S (2004) Anthracene derivative for a non-doped blue-emitting organic electroluminescence device with both excellent color purity and high efficiency. Chem Phys Lett 397:1–4
4. Wen SW, Lee MT, Chen CH (2005) Recent development of blue fluorescent OLED materials and devices. J Disp Technol 1:90–99
5. Huang J, Su JH, Tian H (2012) The development of anthracene derivatives for organic light-emitting diodes. J Mater Chem 22: 10977–10989
6. Xia ZY, Zhang ZY, Su JH, Zhang Q, Fung KM, Lam MK, Li KF, Wong WY, Cheah KW, Tian H, Chen CH (2010) Robust and highly efficient blue light-emitting hosts based on indene-substituted anthracene. J Mater Chem 20:3768–3774
7. Huang J, Su JH, Li X, Lam MK, Fung KM, Fan HH, Cheah KW, Chen CH, Tian H (2011) Bipolar anthracene derivatives containing hole- and electron-transporting moieties for highly efficient blue electroluminescence devices. J Mater Chem 21: 2957–2964
8. Xia ZY, Su JH, Wong WY, Wang L, Cheah KW, Tian H, Chen CH (2011) High performance organic light-emitting diodes based on tetra (methoxy)-containing anthracene derivatives as a hole transport and electron-blocking layer. J Mater Chem 21:8382–8388
9. Shi J, Tang CW (2002) Anthracene derivatives for stable blue-emitting organic electroluminescence devices. Appl Phys Lett 80: 3201–8203
10. Salbeck J, Yu N, Bauer J, Weissörtel F, Bestgen H (1997) Low molecular organic glasses for blue electroluminescence. Synth Met 91:209–215
11. O'Brien DF, Burrows PE, Forrest SR, Konne BE, Loy DE, Thompson ME (1998) Hole transporting materials with high glass transition temperatures for use in organic light-emitting devices. Adv Mater 10:1108–1112
12. Salbeck J, Bauer J, Weissörtel F (1997) Spiro linked compounds for use as active materials in organic light emitting diodes. Macromol Symp 125:121–132
13. Katsuma K, Shirota Y (1998) A novel class of π-electron dendrimers for thermally and morphologically stable amorphous molecular materials. Adv Mater 10:23–26
14. Bach U, Cloedt KD, Spreitzer H, Gratzel M (2000) Characterization of hole transport in a new class of spiro-linked oligotriphenylamine compounds. Adv Mater 12:1060–1063
15. Ko CW, Tao YT (2002) 9,9-Bis[4-[di-(p-biphenyl)aminophenyl]] fluorene: a high Tg and efficient hole transporting material for electroluminescent devices. Synth Met 126:37–41
16. Kim KS, Jeon YM, Kim JW, Lee CW, Gong MS (2008) Blue light-emitting OLED using new spiro[fluorene-7, 9′-benzofluorene] host and dopant materials. Org Electron 9:797–804
17. Jeon SO, Jeon YM, Kim JW, Lee CW, Gong MS (2008) Blue organic light-emitting diode with improved color purity using 5-naphthyl-spiro[fluorene-7,9′-benzofluorene]. Org Electron 9:522–532
18. Kim KS, Jeon YM, Lee HS, Kim JW, Lee CW, Jang JG et al (2008) (2008) Blue organic electroluminescent devices based on the spiro[fluorene-7, 9′-benzofluorene] derivatives as host and dopant materials. Synth Met 158:870–875
19. Jeon YM, Kim JW, Lee CW, Gong MS (2009) Blue organic light-emitting diodes using novel spiro[fluorene-benzofluorene]-type host materials. Dyes Pigments 83:66–71
20. Jeon SO, Jeon YM, Kim JW, Lee CW, Gong MS (2009) Spiro[fluorene-7,9′-benzofluorene] host and dopant materials for blue light-emitting electroluminescence device. Synth Met 159: 1147–1152
21. Kim KS, Lee HS, Jeon YM, Kim JW, Lee CW, Gong MS (2009) Blue light-emitting diodes from 2-(10-naphthylanthracene)-spiro[fluorene-7,9′-benzofluorene] host material. Dyes Pigments 81: 174–179
22. Kim JY, Lee CW, Jang JG, Gong MS (2012) Orange phosphorescent organic light-emitting diodes using new spiro[benzoanthracene-fluorene]-type host materials. Dyes Pigments 94:304–313
23. Kim MJ, Lee CW, Gong MS (2014) New spirobenzoanthracene derivatives with dinaphthylanthracene core: synthesis and application in sky-blue fluorescent host materials. Dyes Pigments 105:202–207
24. Gong MS, Lee HS, Jeon YM (2010) Highly efficient blue OLED based on 9-anthracene spirobenzofluorene derivatives as host materials. J Mater Chem 20:10735–10746
25. Danel K, Huang TH, Lin JT, Tao YT, Chuen CH (2002) Blue-emitting anthracenes with end-capping diarylamines. Chem Mater 14:3860–3865
26. Aziz H, Popovic ZD (2004) Degradation phenomena in small-molecule organic light emitting devices. Chem Mater 16: 4522–4532

27. Kim SK, Yang B, Ma Y, Lee JH, Park JW (2008) Exceedingly efficient deep-blue electroluminescence from new anthracenes obtained using rational molecular design. J Mater Chem 18:3376–3384
28. Cheon JW, Lee CW, Gong MS, Geum N (2004) Chemiluminescent properties of blue fluorophores containing naphthalene unit. Dyes Pigments 61:23–30
29. Jang SE, Joo CW, Yook KS, Kim JW, Lee CW, Lee JY (2010) Thermally stable fluorescent blue organic light-emitting diodes using spirobifluorene based anthracene host materials with different substitution Position. Synth Met 160:1184–1188
30. Lin HP, Zhou F, Zhang XW, Yu DB, Li J, Zhang L, Jiang XY, Zhang ZL (2011) Enhanced color stability and improved performance in white organic light-emitting devices by utilizing a double-graded structure. Synth Met 161:1133–1136
31. Park JK, Lee KH, Kang S, Lee JY, Park JS, Seo JH, Kim YK, Yoon SS (2010) Highly efficient blue-emitting materials based on 10-naphthylanthracene derivatives for OLEDs. Org Electron 11:905–915
32. Adachi C, Baldo MA, Thopmson ME, Forrest SR (2001) Nearly 100 % internal phosphorescence efficiency in an organic light-emitting device. J Appl Phys 90:5048–5051